Inorg. Chem. **2006**, *45*, 3606–3612

Multiple Bicyclic Diamide–Lutetium Complexes in Solution: Chemometric Analysis of Deep-UV Raman Spectroscopic Data

Victor A. Shashilov, Vladimir V. Ermolenkov,† and Igor K. Lednev*

Department of Chemistry, University at Albany, State University of New York (SUNY), 1400 Washington Avenue, Albany, New York 12222

Received January 6, 2006

The investigation of complex formation between a bicyclic diamide, a novel chelating agent for lanthanides and actinides, and lutetium in an acetonitrile solution is reported. A free ligand and its lutetium complexes showed weak, noncharacteristic near-UV absorption and no fluorescence, which limited the application of absorption and fluorescence spectroscopies for studying this system. Deep-UV Raman spectroscopy combined with chemometric analysis was shown to be a powerful tool for quantitative characterization of multiple equilibria between lutetium and a bicyclic diamide. Several chemometric methods were utilized for a comparative analysis of Raman spectroscopic data. It was found that a recently developed stepwise maximum angle calculation algorithm followed by alternative least squares (ALS) was more efficient than the commonly used combination of evolving factor analysis and ALS methods, especially when little or no information about the system composition and the spectra of individual components was available. A free ligand and 1:1, 1:2, and 1:3 metal–ligand complexes were distinguished in a bicyclic diamide–lutetium solution. The composition evolution of the solution during the course of titration with lutetium was described, and the stepwise stability constants of complex formation, $K_1{:}K_2 = 0.80 \pm 0.15$ ($K_{1,2} > 10^8$ M^{-1}) and $K_3 = (5.5 \pm 1) \times 10^3$ M^{-1}, were estimated.

Introduction

A detailed structural understanding of metal−ligand complexes in solution is important for developing novel efficient catalysts, metal-extracting ligands, metal-sensing elements, etc. X-ray crystallography provides the most accurate structural information, yet the composition of the complexes in crystalline form and in solution might be different. Multidimensional NMR spectroscopy allows for elucidation of a molecular structure in solution with atomic resolution in many cases. However, ^{13}C and ^{17}O NMR spectra, which would be the most informative for diamide chelate complexes, have intrinsic sensitivity limitations because of the low natural abundance and small gyromagnetic ratios of ^{13}C and ^{17}O.[1,2] Raman spectroscopy has been extensively used for studying the structure of metal−ligand complexes[3] and a chemical equilibrium in solutions of coordination compounds.[4] In the case of multiple equilibria, multivariate spectral analysis has been applied for determining stepwise stability constants with no a priori information about the number of spectroscopically distinguishable species and their stoichiometries.[4,5] Resonance Raman spectroscopy has been proven to be the most valuable for structural studies because (i) the spectra are simplified in this case as a result of the resonance enhancement of selected vibrational modes only and could be predicted based on molecular modeling[6−8] and (ii) the sensitivity of Raman spectroscopy is strongly increased as a result of the resonance enhancement. Not all ligands and their metal complexes exhibit absorption in the visible and near-UV spectral regions, which limits the application of traditional Raman spectroscopy. We have recently utilized deep-UV resonance Raman (DUVRR)

* To whom correspondence should be addressed. E-mail: lednev@albany.edu. Fax: (518) 442-3462.
† Also affiliated with B. I. Stepanov Institute of Physics, National Academy of Sciences of Belarus, Minsk, Belarus.

(1) Webb, A. G. *J. Pharm. Biomed. Anal.* **2005**, *38*, 892−903.
(2) Zhu, X.-H.; Zhang, Y.; Tian, R.-X.; Lei, H.; Zhang, N.; Zhang, X.; Merkle, H.; Ugurbil, K.; Chen, W. *Proc. Natl. Acad. Sci. U.S.A.* **2002**, *99*, 13194−13199.
(3) Nakamoto, K. *Infrared and Raman Spectra of Inorganic and Coordination Compound Part. B. Applications in coordination, organometallic, and bioinorganic chemistry*, 5th ed.; John Wiley & Sons, Ltd.: New York, 1997.
(4) Uibel, R. H.; Harris, J. M. *Anal. Chem.* **2005**, *77*, 991−1000.
(5) Tomisic, V.; Simeon, V. *Phys. Chem. Chem. Phys.* **2000**, *2*, 1943−1949.
(6) Asher, S. A. *Anal. Chem.* **1993**, *65*, 201A−210A.
(7) Asher, S. A. *Anal. Chem.* **1993**, *65*, 59A−66A.
(8) Asher, S. A. *Annu. Rev. Phys. Chem.* **1988**, *39*, 537−588.

10.1021/ic0600331 CCC: $33.50
Published on Web 03/30/2006

spectroscopy combined with molecular modeling for structural characterization of Lu^{III} and La^{III} complexes with a bicyclic diamide **1** under saturation with metal ions.[9]

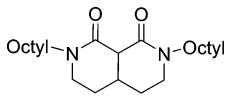

1

This novel chelating agent for lanthanides and actinides exhibits a strong absorption band around 200 nm that enables strong resonance enhancement of Raman scattering at 197-nm excitation. The obtained results have demonstrated a strong intrinsic sensitivity and selectivity of the Raman spectroscopic signature of the ligand. Molecular modeling, which included structure optimization and calculation of Raman frequencies and resonance intensities, allowed for assignment of all strong Raman bands of the bicyclic diamide as well as prediction of the band shifts observed as a result of complex formation with metal ions. A comparative analysis of Raman spectra and the results of the molecular modeling could be used for elucidation of the structure of complexes in solution. Here we report on the first application of DUVRR spectroscopy combined with chemometric analysis for characterization of the composition of ligand−metal ion complexes at various stages of complex formation.

Experimental Section

Materials and Sample Preparation. Ligand octyl **1** was kindly provided by Prof. James Hutchison and Bevin W. Parks, University of Oregon, Eugene, OR. $Lu(CF_3SO_3)_3$ (Aldrich) and **1** were dehydrated in a vacuum centrifuge and then dissolved in acetonitrile (Aldrich, spectrophotometric grade) previously dried with silica gel (Davisil 633).

Spectral Measurements. DUVRR instrumentation has been described in detail elsewhere.[10] Briefly, a 197-nm laser beam (∼1 mW, Indigo-S laser system from Coherent) was focused into a spinning Suprasil NMR tube (5-mm outer diameter; 0.38-mm wall thickness) containing 150 μL of solution. To avoid sample heating, the solution was additionally mixed using a magnetic stirrer. Scattered radiation was collected in backscattering geometry, dispersed using a home-built double monochromator, and detected with a liquid-nitrogen-cooled CCD camera (Roper Scientific). The accumulation time for every spectrum was 6 min. GRAMS/AI(7.01) software was used for Raman spectroscopic data processing. Raman spectra were normalized using acetonitrile as an internal standard. The contribution of Suprasil and acetonitrile scattering to Raman spectra was quantitatively subtracted.

Chemometric Analysis. The chemometric analysis was performed using PLS_Toolbox 3.5 (Eigenvector Research, Manson, WA)[11] and homemade programs operating in the *Matlab* environment. Principal component analysis (PCA), evolving factor analysis (EFA), and multivariate curve resolution (MCR) were consequently employed as described by Potyrailo.[12] Various baseline correction[11] and smoothing[13] methods were exploited to prepare Raman spectra for the PCA.[14]

A baseline is known to increase the effective rank of the data matrix.[5] Consequently, a proper choice of a baseline correction method could significantly improve subsequent factor analysis.[15] We utilized linear and parabolic approximations using PLS_ToolBox 3.5 functions.[11] It turned out that both approximations gave satisfactory results; however, in the case of the parabolic approximations, the secondary eigenvalues were higher, which made linear approximations preferable for the set of Raman spectra analyzed here.

We utilized the Savitzky−Golay smoothing method[13] with a five-point filter window and second-order polynomials for the smoothing of Raman spectra. The sharpness of the Raman peaks did not allow for use of a wider smoothing window without distortion of the spectrum profiles. Low-pass fast Fourier transform (FFT) filtering was found to provide no appreciable improvement in terms of either eigenvalue ratios or cumulative variance covered by primary factors. Consequently, Savitzky−Golay smoothing was more appropriate for our data. However, in general, the adequate choice of parameters of smoothing such as a smoothing window, order of polynomials in the Savitzky-Golay method, or cutoff frequency in FFT could be important.

Abstract factor analysis (AFA) was performed on the set of Raman spectra and covariance matrixes using algorithms described by Malinowski[14] and PLS_Toolbox functions.[11] Three scaling methods, mean centering,[16] covariance about the origin (nonscaling),[17] and autoscaling,[18] were tested to prepare the data for AFA, specifically, to find the number of significant components. On the whole, all three preprocessing methods suggested the presence of four significant components. Nevertheless, the parameters obtained based on nonscaled and mean-centered matrixes such as eigenvalue ratios, autocorrelation coefficients,[14] and the residual-mean-squared-error-of-cross-validation (RMSECV)[14,19] were more consistent and easier to interpret. The latter allowed us to conclude that nonscaling and mean centering were more appropriate for Raman data. In fact, mean centering and nonscaling lead to data where the wavenumbers with large intensity variations are given higher weights, while autoscaling treats the wavenumbers with high and low intensity variations as equally important.[11] This is probably why mean centering and nonscaling are more appropriate for spectroscopic data, in particular for DUVRR spectral sets.

The EFA[5] followed by alternative least-squares (ALS) analysis[17] was applied for estimation of the spectra of individual components and their concentrations. At this stage, nonnegative and equality constraints[20,21] were imposed on the concentration matrix. The equality constraints were used to set the total concentration of the ligand at all titration points to the initial concentration of the ligand.

(9) Shashilov, V. A.; Ermolenkov, V. V.; Levitskaia, T. G.; Lednev, I. K. *J. Phys. Chem. A* **2005**, *109*, 7094−7098.
(10) Lednev, I. K.; Ermolenkov, V. V.; He., W.; Xu, M. *Anal. Bioanal. Chem.* **2005**, *381*, 431−437.
(11) Wise, B. M.; Gallagher, N. B.; Bro, R.; Shaver, J. M.; Windig, W.; Koch, R. S. *PLS_Toolbox 3.5 for Use with Matlab*; Eigenvector Research, Inc.: Manson, WA, 2005.
(12) Potyrailo, R. A. *Trends Anal. Chem.* **2003**, *22*, 374−384.
(13) Chan, F.; Liang, Y.; Gao, J.; Shao, X. *Chemometrics: from Basics to Wavelet Transform*; NIR Publications: Hoboken, NJ, 2004.
(14) Malinowski, E. R. *Factor Analysis in Chemistry*, 3rd ed.; John Wiley & Sons: New York, 2002.
(15) Shaver, J. M. In *Handbook of Raman Spectroscopy: From the Research Laboratory to the Process Line*; Lewis, I. R., Edwards, H. G. M., Eds.; Marcel Dekker: New York, 2001; p 281.
(16) Cooper, J. B. *Chemom. Intell. Lab. Syst.* **1999**, *46*, 231−247.
(17) Garrido, M.; Lazaro, I.; Larrechi, M. S.; Rius, F. X. *Anal. Chim. Acta* **2004**, *515*, 65−73.
(18) Svensson, O.; Josefson, M.; Langkilde, F. W. *Chemom. Intell. Lab. Syst.* **1999**, *49*, 49−66.
(19) Navea, S.; Tauler, R.; de Juan, A. *Anal. Biochem.* **2005**, *336*, 231−242.
(20) Gemperline, P. J.; Cash, E. *Anal. Chem.* **2003**, *75*, 4236−4243.
(21) Jaumota, J.; Gargalloa, R.; de Juan, A.; Tauler, R. *Chemom. Intell. Lab. Syst.* **2005**, *76*, 101−110.

These constraints were applied in the form of a penalty function during the ALS fit. The individual component spectra were restricted to positive values. We also required that the spectrum of the first significant component be equal to the known spectrum of the free ligand. *Matlab* functions, which impose soft constraints[20] on spectra and concentrations during the ALS search, are given in the Supporting Information.

As an alternative to EFA and ALS, pure variable methods[22] were utilized for the chemometric analysis. In particular, we implemented a recently developed stepwise maximum angle calculation[23] (SMAC) algorithm and compared it with the SIMPLISMA[24] (simple-to-use interactive self-modeling mixture analysis) approach. For SIMPLISMA and SMAC algorithms, we used second-derivative spectra because they had sharper and better-resolved peaks, which eliminated the overlap problems.[24]

It is also possible to use second-derivative spectra for ALS fitting if only concentrations rather than both spectra and concentrations are positively constrained. Because differentiation is a linear operation, the concentration profiles should be the same whether they are obtained based on the second-derivative data set or conventionally, i.e., as recorded spectra.[25] Once the concentration profiles are calculated, the pure-component spectra can be readily resolved based on those profiles and the conventional spectral set using nonnegative ALS.

Our study showed that both SMAC and SIMPLISMA approaches led to the same resolved spectral and concentration profiles. Moreover, the spectral and concentration curves obtained by SMAC and SIMPLISMA were close to those obtained by the combination of EFA and ALS. However, in the case of SMAC and SIMPLISMA, the concentration curves had small negative values at some titration points. As the next step, the spectral and concentration profiles obtained by SMAC and SIMPLISMA were constrained to nonnegative values and refined by ALS. The *Matlab* code of the SMAC algorithm is provided in the Supporting Information.

In addition, the performance of SMAC followed by the ALS algorithm was compared with that of the combination of EFA and ALS algorithms using spectral sets of simulated Raman spectra of multicomponent mixtures. The simulated spectra of the individual components were strongly overlapping; the concentrations of all components in various samples were generated as either random numbers or smooth multiple peak profiles with random shapes. Then the spectrum for each sample was obtained based on the simulated pure-component spectra and their concentrations. Finally, random noise and a baseline were added to the simulated spectrum of each sample. Because of the presence of randomly distributed multiple peaks in the concentration profiles of each species, EFA was unable to extract any information about the shapes of the concentration curves. Under such conditions, ALS with nonnegative constraints on spectra and concentrations failed to reconstruct spectra of individual components in most cases. This is because of the well-known ambiguity of this method.[26] In contrast to ALS, the SMAC approach resolved the simulated spectral sets into individual component spectra reasonably well, although minor negative regions in the resolved spectral and concentration profiles appeared in some cases. To eliminate those negative regions, the spectra and concentrations resolved by SMAC were used as starting points for nonnegative ALS fitting. The simulations showed that the SMAC algorithm is particularly suitable for the analysis of multicomponent systems in which the concentrations of the components change in a complex or irregular fashion and no a priori information about the spectra and concentrations of the components is available. In addition, it can provide a good initial guess for conventional MCR methods.

Results and Discussion

Titration of 1 with Lu^{III}: Raman Spectroscopy and Chemometric Analysis. Titration of the acetonitrile solution of **1** with $Lu(CF_3SO_3)_3$ was performed according to the molar ratio scheme; i.e., the total concentration of **1** was held constant and equal to 1.5 and 7.5 mM in the first and second titration experiments, respectively. In each experiment, DUVRR spectra were recorded at 11 titration points with 0.0, 0.05, 0.1, 0.15, 0.3, 0.6, 0.75, 1.0, 3.0, 6.0, and 12.0 mM $Lu(CF_3SO_3)_3$ to produce 21 different Raman spectra. Two spectra, 0.1 and 3.0 mM, in the first titration were eliminated as outliers at the early stage of chemometric analysis. Figure 1 shows resonance Raman spectra of bicyclic diamide **1** in acetonitrile obtained at various stages of titration with $Lu(CF_3SO_3)_3$. All Raman bands of ligand **1** have been assigned based on molecular modeling.[9] Several changes in the Raman spectrum of **1** were evident in various concentration ranges of $Lu(CF_3SO_3)_3$, which indicated the formation of several types of ligand−Lu complexes. In particular, the 1672-cm^{-1} amide I band gradually decreased as new bands at 1602 and 1514 cm^{-1} appeared at high salt concentrations. As is evident from Figure 1, the appearance of a new 1636-cm^{-1} band was shifted to the higher Lu concentrations (see also Figures 1 and 2 in the Supporting Information).

Comprehensive chemometric analysis of DUVRR spectra of **1** measured at various concentrations of $Lu(CF_3SO_3)_3$ was performed for (i) determination of the number of various ligand−metal complexes formed in the course of titration, (ii) determination of their concentrations at each titration point, (iii) calculation of DUVRR spectra, and (iv) calculation of stability constants for each ligand−metal complex. AFA (utilizing three different scaling methods; see the Experimental Section) was performed on 21 Raman spectra of **1** obtained in two Lu titration experiments described above.

The concentrations (Figure 2) and spectra of individual components (Figure 3) at various stages of titration were obtained using the EFA[5] followed by ALS analysis.[17] To obtain physically meaningful values of the concentrations at each titration step, the calculated concentrations were scaled so that the initial concentration of the ligand is equal to 0.15 mM.

The chemometric analysis of 21 DUVRR spectra allowed us to determine the number of significant components, the pure-component spectra, and the concentration profiles for the significant components. However, we used only nine Raman spectra recorded in the first titration experiment (1.5 mM ligand concentration) for determination of the stability constants. A total of 36 concentration points (nine-point concentration profile for each of four resolved species) were

(22) Windig, W. *Chemom. Intell. Lab. Syst.* **1997**, *36*, 3−16.
(23) Windig, W.; Gallagher, N. B.; Shaver, J. M.; Wise, B. M. *Chemom. Intell. Lab. Syst.* **2005**, *77*, 85−96.
(24) Windig, W.; Antalek, B.; Lippert, J. L.; Batonneau, Y.; Bremard, C. *Anal. Chem.* **2002**, *74*, 1371−1379.
(25) Astakhov, S. A.; Stoegbauer, H.; Kraskov, A.; Grassberger, P. Preprint submitted to *Chemom. Intell. Lab. Syst.*, 2006.
(26) Leger, M. N.; Wentzell, P. D. *Chemom. Intell. Lab. Syst.* **2002**, *62*, 171−188.

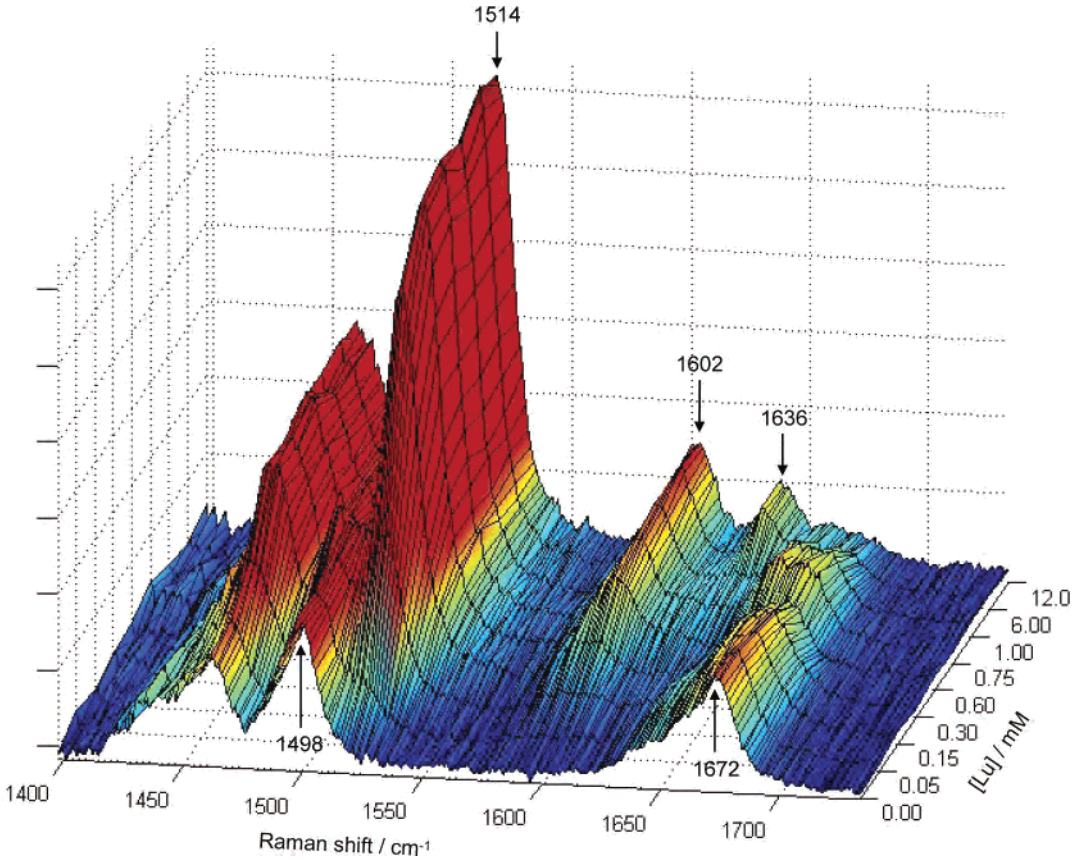

Figure 1. 197-nm resonance Raman spectrum of **1** (1.5 mM) in acetonitrile at various concentrations of $Lu(CF_3SO_3)_3$.

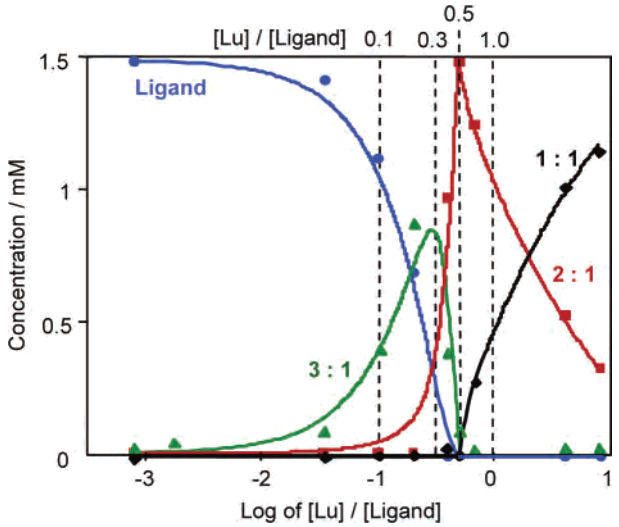

Figure 2. Solution composition at various stages of titration with $Lu(CF_3SO_3)_3$. Markers show concentrations of **1** (blue) and its 3:1 (green), 2:1 (red), and 1:1 (black) Lu complexes reconstructed by chemometrics; solid lines represent the best fit.

fitted simultaneously to estimate three stability constants. Because of the large concentration of the ligand in the second titration experiment (7.5 mM ligand concentration), the contributions of 2:1 and 1:1 complexes became noticeable only at the two highest concentrations of Lu. This made fitting of the concentration profiles reconstructed based on the second titration impractical.

Figure 2 shows the concentration profiles for four individual species identified by the chemometric treatment of Raman spectral data obtained in the first titration experiment. Similar shapes of concentration profiles were obtained from the analysis of the spectra recorded in the second titrations (data not shown), except the contributions of 2:1 and 1:1 complexes became noticeable only at the two last titration points because of a high ligand concentration. It was straightforward to assign the first species dominating at low $Lu(CF_3SO_3)_3$ concentrations to the free ligand **1**. The concentration of the free ligand decreases as more metal is added and approaches zero at ~0.6 mM salt concentration, i.e., when the ligand−metal concentration ratio is about 3:1. This indicates the formation of a 3:1 complex with a high stability constant. The same extraction stoichiometry, i.e., three molecules of extractant bound to a metal ion of lanthanides (Eu) and actinides (Am), has been reported for ligand **1** previously.[27,28] The concentration profile of the third species exhibiting a maximum at 0.75 mM Lu (2:1 ligand−metal ion concentration ratio) could be preliminarily assigned to the 2:1 ligand−metal complex. The ability to coordinate lanthanides with 2:1 stoichiometry has been recently reported for the methyl derivative of **1**.[29] A further increase in the concentration of Lu^{III} gave rise to the formation of the fourth species, which was tentatively assigned to the 1:1 complex.

(27) Sinkov, S. I.; Rapko, B. M.; Lumetta, G. J.; Hay, B. P. *Inorg. Chem.* **2004**, *43*, 8404−8413.
(28) Lumetta, G. J.; Rapko, B. M.; Hay, B. P.; Garza, P. A.; Hutchison, J. E.; Gilbertson, R. D. *Solvent Extr. Ion Exch.* **2003**, *21*, 29−39.
(29) Lumetta, G. J.; Rapko, B. M.; Garza, P. A.; Hay, B. P.; Gilbertson, R. D.; Weakley, T. J. R.; Hutchison, J. E. *J. Am. Chem. Soc.* **2002**, *124*, 5644−5645.

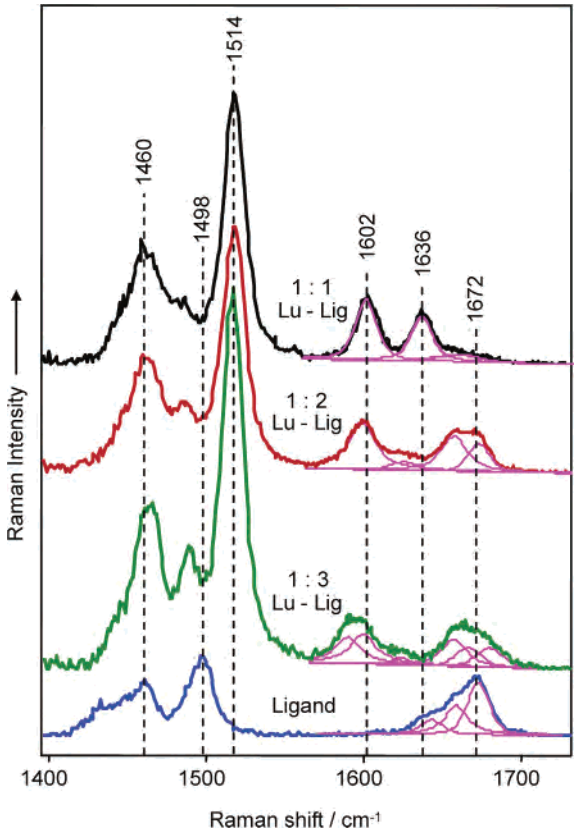

Figure 3. Raman spectra of the free ligand and its Lu complexes reconstructed using chemometric analysis.

Even at 8-fold excess of metal ions, ~20% of the ligand was present in the form of L_2M complexes.

Stepwise Stability Constants of Complex Formation. A general approach[30] for reactions of multiple complex formation was utilized for determination of the stability constants (see the Supporting Information for details). A homemade *Matlab* program implementing the simplex method for extracting the stability constants (Supporting Information) resulted in determination of the stepwise stability constant for the 3:1 complex, $\log(K_3) = 3.73$, and the ratio of constants for 1:1 and 2:1 complexes, $K_1{:}K_2 = 0.8$. However, the $K_2{:}K_3$ ratio needed for a complete set of the stability constants could not be unambiguously retrieved from our data. The estimation of K_3 was based on the free ligand concentration, which can be confidently found at the early stage of titration (Figure 2). On the other hand, the $K_1{:}K_2$ ratio was evaluated from the fractions of 2:1 and 1:1 complexes at metal ion concentrations exceeding the total concentration of the ligand. The $K_2{:}K_3$ ratio could not be determined because all fitting curves did not change when the values for K_1 and K_2 varied in the range of 10^8-10^{22} M^{-1} if the $K_1{:}K_2$ ratio was kept constant (Supporting Information). The fitting became worse when K_1 and K_2 were smaller than 10^6 M^{-1}. Therefore, the relation $K_1 \sim K_2 \gg K_3$ was established for the stepwise stability constants. This explains why the 2:1 complex dominated at the salt concentration of 0.75 mM (Figure 2).

(30) Meites, L. *An introduction to chemical equilibrium kinetics*; Pergamon Press: New York, 1981.

The solid curves in Figure 2 calculated at $\log(K_3) = 3.73$, $\log(K_1) = 14$, and $K_1{:}K_2 = 0.8$ showed a good agreement with the concentration profiles determined from chemometrics. It is important to note that the calculated chemometric concentration profiles were obtained with no physical assumption about the reaction scheme, resulting in equilibrium between different species. A good agreement between the chemometrics results, and the fitting based on the chemical reaction scheme confirmed the validity of the employed approaches and the reliability of the data obtained.

The concentration profile for the 2:1 complex shown in Figure 2 exhibits an apparent break when the concentration of metal approached half of the total ligand concentration. Note that the break profile is straightened by the logarithmic scale chosen for the metal concentration. In excess of free ligand at the initial stage of titration, the 3:1 complex dominated. As soon as most ligand molecules were bound by Lu ions to form 3:1 complexes (i.e., the ligand−metal concentration ratio was of about 3:1), the equilibrium in the solution became controlled by the competition between the 3:1 and 2:1 complexes. Because the formation constant for the 2:1 complex is at least 4 orders of magnitude higher than that of the 3:1 complex, the concentration of the former rose abruptly, as is evident from the steep slope of the corresponding concentration profile. Because $K_1 \sim K_2$ and $K_{1,2} \gg K_3$, no 1:1 complexes form until the total metal concentration reaches half of the total ligand concentration. However, right after this point (the metal concentration equals half of the total ligand concentration), the concentration of 1:1 complexes increases and that of 2:1 complexes decreases almost linearly with the metal concentration. This results in sharp breaks in the concentration profiles for all individual complexes. Somewhat similar breaks of the concentration profiles have been reported by Uibel and Harris.[4] Note that Figure 10a in the referenced work[4] shows a 3-fold concentration change only, while our Figure 2 illustrates a 4 order of magnitude change because of the logarithmic scale, which further strengthens the sharpness of the breaks.

Determination of the confidence interval for the estimated stability constants was complicated by the fact that the chemometric data instead of directly measured experimental data were fitted. We employed a Monte Carlo simulation for verifying the robustness of the estimated parameters. This method has been reported for estimation of the confidence intervals for stability constants found from spectroscopy data.[31] In our study, the chemometric curves were spoiled with a predefined random error. The standard error was estimated from the standard deviation of the concentration profiles calculated during the ALS fit. Then the spoiled data set was fitted, and new best-fit parameters were determined. Comparing the new parameters with those for the original data allowed for conclusions about the sensitivity of the estimated parameters to the error in the chemometric model. A total of 25 000 spectra were constructed for the Monte Carlo simulation, and 95% confidence intervals for K_3 and $K_1{:}K_2$ ratios were found from the frequency distribution

(31) Alper, J. S.; Gelb, R. I. *J. Phys. Chem.* **1991**, *95*, 104−108.

functions.[32] Standard errors were then derived using coefficients of the Student's *t* distribution[31,33] to give $K_3 = (5.5 \pm 1.0) \times 10^3\ M^{-1}$ and $K_1{:}K_2 = 0.80 \pm 0.15$.

Raman Spectra of Ligand−Lu Complexes. The Raman spectra of individual components resolved by the ALS and SMAC analyses are shown in Figure 3. The high-frequency bands in the spectra were fitted with the minimum number of peaks. As is evident from the experimental spectrum of the free ligand, its high-frequency DUVRR band is broad and contributed by at least three components. In fact, fitting this band with three Gaussian contours reproduced the band shape with the accuracy of the experimental noise. The widths of the Gaussian peaks were estimated to fall into the range of 18−21 cm^{-1}. On the other hand, both high-frequency bands in the calculated spectrum of the 1:1 complex were sharp and either band was accurately fitted with a single Gaussian profile of 20-cm^{-1} width. As a first approximation, the high-frequency bands of the 3:1 and 2:1 complexes were fit with a combination of Gaussian peaks with a bandwidth within the range of 18−21 cm^{-1}. It turned out that the amide bands of the 3:1 and 2:1 complexes could be fitted satisfactorily with three and two Gaussian profiles, respectively, as shown in Figure 3. Consequently, the spectrum of the 1:1 complex mainly required two peaks only for fitting of the amide I bands. The rest of the spectra required several peaks for fitting of broad amide I bands, which, most probably, indicated the presence of multiple conformations.

The spectra of individual components could be used potentially for characterization of the structure of species formed in solution. The spectrum of the first species was, as expected, identical with the spectrum of the free ligand. The amide I band in the spectrum was broad and consisted of at least three overlapping peaks. Most probably, a free ligand adopted more than one conformation in solution. The existence of several possible conformers has been predicted by MM2 modeling for bicyclic diamides.[29] In particular, the cis and trans conformers had different dihedral angles between the planes containing the C═O moieties. The latter might result in different vibrational interactions between C═O stretchings in different conformers and might ultimately lead to a complex amide I band in the free-ligand Raman spectrum.

The Raman spectrum of the 1:1 complex is close to the spectrum of the ligand−Lu complex formed with an excess of Lu salt in solution reported recently.[9] The downshift of the amide I band in the spectrum of the 1:1 complex has been attributed to the elongated and weakened C═O bonds of the ligand in the complexed form.[9] A strengthened coupling of the C−N and C═O stretching vibrations predicted by ab initio calculation leads to a further downshift of the amide I band as a result of the increased contribution of C−N stretching to the amide I normal mode. The presence of a strong 1514-cm^{-1} band in the 1:1 complex spectrum was consistent with our previous experimental observations and ab initio calculations.[9] This band was assigned to the strengthened coupling of C═O and C−C_αH stretching vibrations from two hydrocarbon rings in the complex. The sharpest 1498-cm^{-1} band in the spectrum of the free ligand was obscured and downshifted in the 1:1 complex. Such an intensity decrease can be explained by the constrained C−N stretching in the diamide−Lu complex.[9] The ligand moiety in the 1:1 complex most probably adopted a single conformation, which was evident from the increased sharpness and apparent "splitting" of the amide I band (Figure 3).

Raman spectra of 3:1 and 2:1 complexes showed two broad bands centered at 1600 and 1670 cm^{-1} (Figure 3). An ab initio study of 3:1 and 2:1 complexes was not completed by this time because of the complexity of the molecules. Because of the low symmetry of the complexes, the normal modes of each ligand in the complex might have different frequencies, leading to the broadening of the Raman bands. A complicated vibrational structure of the high-frequency modes of 2:1 and 3:1 complexes can be associated with the difference in the local geometries of the coordinating ligands. X-ray data for the 2:1 complex of the methyl derivative of **1** (instead of octyl) with Eu have shown a significant distortion of the ligands after complex formation.[29] In particular, the C═O bond lengths have been found to be 1.241 and 1.246 Å for one ligand and 1.224 and 1.260 Å for the other one in the complex. Such differences in the bond lengths in the complex could result in the separation of the corresponding high-frequency modes. Alternatively, the presence of several conformers of 2:1 and 3:1 complexes in solution could also result in the broadening of the high-frequency Raman bands. It is worth mentioning here that rotational ambiguity could affect amide I bands in the resolved spectra of 2:1 and 1:1 complexes and could result in the mixing of higher frequency bands in the pure spectra of these two complexes. It is difficult to completely avoid such a mixing between close or highly overlapping spectra even when second-derivative spectra are used at the initial stage of the analysis. However, the widths of the amide I bands in the calculated spectra seem to be reasonable taking into account the broad amide I band in the experimental spectrum of the free ligand and the diversity of conformations adopted by ligand molecules in the multiple complexes. Clearly, there is more structural information about the free ligand and complexes in their Raman spectra than we can retrieve at this time. A further study will be required to make a meaningful assignment for the individual components in the fitted Raman spectra.

Conclusions

DUVRR spectroscopy combined with multivariate spectral analysis was demonstrated to be a powerful tool for characterization of the composition of ligand−metal ion complexes in solution. The analysis of the 197-nm excited Raman spectra allowed for the distinguishment of four components attributed to the free ligand and 1:1, 1:2, and 1:3 metal−ligand complexes. The corresponding equilibrium constants of complex formation, $K_1{:}K_2 = 0.8 \pm 0.15$ ($K_{1,2}$

(32) Christopoulos, A. *Trends Pharmacol. Sci.* **1998**, *19*, 351−357.
(33) Motulsky, H.; Christopoulos, A. *Fitting Data to Biological Data Using Linear and Nonlinear Regression: a practical guide to curve fitting*; GraphPad Software, Inc.: San Diego, 2003.

$> 10^8$ M^{-1}) and $K_3 = (5.5 \pm 1) \times 10^3$ M^{-1}, were estimated by fitting of the component concentration profiles. Significantly smaller stability constants ($K_1 \sim 65$ M^{-1}, $K_2 \sim 13$ M^{-1}, and $K_3 \sim 1.4$ M^{-1}) have been reported for the Am complexes of the methyl-substituted analogue of **1** in an acidic nitrate aqueous solution.[27] Similarly to our results, the 3:1 complex has the smallest stability constant while the K_1 and K_2 constants are of the same order. The next challenge of this project is to elucidate the structure of the identified $\mathbf{1}_x$−Lu complexes by comparing the Raman spectroscopic signatures found from chemometric analysis with spectra predicted by molecular modeling and to estimate the absolute values of the equilibrium constants K_1 and K_2.

A newly developed SMAC method followed by ALS was compared with a common approach of using EFA followed by ALS methods in order to deconvolve the DUVRR data set into the spectra of individual components and their concentrations. The MCR methods alone are of limited use for such types of problems unless a good initial estimation based on the knowledge of the system under study is available. EFA is normally utilized for obtaining a proper starting point to MCR. EFA gives only some rough estimation of the regions where the species start to exist and vanish. On the contrary, the initial guess provided by the SMAC method gave crude concentration curves and spectra of individual species, so that only a small amendment was needed to eliminate low-intensity negative regions using nonnegative ALS. Therefore, the initial guess obtained from SMAC is much better and closer to the final spectra than that obtained by EFA. Using SMAC allowed for a combination of two steps of the curve resolution problem: (i) obtaining the initial guess and (ii) resolving spectral and concentration profiles reasonably well. SMAC is fast because it does not perform fitting iteratively. Elimination of low-intensity negative regions of spectra using ALS is then straightforward and much faster than it would be in the case of the initial guess obtained from, e.g., EFA. Consequently, in the case of problems with limited prior information, SMAC combined with ALS is faster and more efficient as compared to the combination of EFA and ALS, which is commonly used for such types of problems.

Acknowledgment. We gratefully acknowledge Prof. James E. Hutchison and Bevin W. Parks from the University of Oregon, Eugene, OR, for providing ligand **1**.

Supporting Information Available: Details on the calculation of the stability constants, a *Matlab* source code for the determination of the stability constants based on chemometric data, *Matlab* functions for the ALS algorithm with soft constraints on spectra and concentrations, and the code for the SMAC algorithm. This material is available free of charge via the Internet at http://pubs.acs.org.

IC0600331